0013-7227/07/$15.00/0
Printed in U.S.A.

Endocrinology 148(4):1736–1744

doi: 10.1210/en.2006-1153

Neuroendocrine Plasticity in the Anterior Pituitary: Gonadotropin-Releasing Hormone-Mediated Movement *in Vitro* and *in Vivo*

Amy M. Navratil, J. Gabriel Knoll, Jennifer D. Whitesell, Stuart A. Tobet, and Colin M. Clay

Department of Reproductive Medicine (A.M.N.), University of California, San Diego, La Jolla, California 92093; and Department of Biomedical Sciences (J.G.K., J.D.W., S.A.T., C.M.C.), Colorado State University, Fort Collins, Colorado 80523

The secretion of LH is cued by the hypothalamic neuropeptide, GnRH. After delivery to the anterior pituitary gland via the hypothalamic-pituitary portal vasculature, GnRH binds to specific high-affinity receptors on the surface of gonadotrope cells and stimulates synthesis and secretion of the gonadotropins, FSH, and LH. In the current study, GnRH caused acute and dramatic changes in cellular morphology in the gonadotrope-derived αT3-1 cell line, which appeared to be mediated by engagement of the actin cytoskeleton; disruption of actin with jasplakinolide abrogated cell movement and GnRH-induced activation of ERK. In live murine pituitary slices infected with an adenovirus-containing Rous sarcoma virus-green fluorescent protein, selected cells responded to GnRH by altering their cellular movements characterized by both formation and extension of cell processes and, surprisingly, spatial repositioning. Consistent with the latter observation, GnRH stimulation increased the migration of dissociated pituitary cells in transwell chambers. Our data using live pituitary slices are a striking example of neuropeptide-evoked movements of cells outside the central nervous system and in a mature peripheral endocrine organ. These findings call for a fundamental change in the current dogma of simple passive diffusion of LH from gonadotropes to capillaries in the pituitary gland. (*Endocrinology* 148: 1736–1744, 2007)

OVULATION IS A FUNDAMENTAL event in reproduction. It requires a dramatic 20- to 30-fold surge of LH released by the anterior pituitary into the peripheral circulation to complete follicular maturation and induce the release of the oocyte from a preovulatory follicle (1). The secretion of LH from the pituitary is cued by the hypothalamic decapeptide, GnRH (2, 3). Secretion of GnRH from hypothalamic neurons and its interpretation by gonadotropes in the pituitary are essential events for reproductive competence in virtually all vertebrates (4).

Gonadotropes are characterized by their ability to mount a cyclical pattern of hormone secretion that culminates in the production of the preovulatory LH surge (5). These cells display structural and functional plasticity throughout the female reproductive cycle reflected as changes in the intracellular stores of LH and FSH, the relative abundance of secretory granules (6), and process extensions in selected cells within the pituitary at particular times during the estrous cycle (7–10). Also, gonadotropes may not be a homogeneous population of cells; the percentage of small, medium, and large or monohormonal and bihormonal gonadotropes may differ according to stage of cycle (6, 9).

The GnRH receptor (GnRHR) is in the superfamily of heptahelical G protein-coupled receptors. Upon ligand activation, agonist-occupied GnRHR couples to $G\alpha_{q/11}$, leading to stimulation of phospholipase C, formation of inositol 1,4,5-trisphosphate and diacylglycerol, elevation of intracellular free calcium, and activation of one or more isoforms of protein kinase C (11, 12). These early events underlie GnRH activation of ERK (13–15). More recently GnRH signaling to MAPK appears to require localization of the GnRHR to low-density membrane microdomains termed lipid rafts (16). It is also interesting that GnRH signaling to ERK in HEK293 cells appears to require actin polymerization (17).

Given the central role of GnRH in reproduction, significant attention has been devoted to understanding the molecular and cellular events that culminate in the biological responses mediated by GnRHR. In the present study, we used an image-based approach to examine GnRH-evoked cell movements in the gonadotrope derived αT3-1 cell line, dissociated pituitary cells, and finally live pituitary slices. Live video microscopy experiments reveal that selected cells in dissociated pituitaries and live pituitary slices respond to GnRH by altering movements reflected as both changes in spatial positioning and formation of cellular processes. These data directly demonstrate neuropeptide-evoked movements of cells outside the central nervous system in a peripheral endocrine organ in real time.

First Published Online January 11, 2007

Abbreviations: CLSM, Confocal laser-scanning microscopy; DIC, differential interference contrast; eGFP, enhanced GFP; GFP, green fluorescent protein; GnRHR, GnRH receptor; ICC, immunocytochemistry; Jas, jasplakinolide; MMP, matrix metalloproteinase; PMA, phorbol 12-myristate-13-acetate; RSV, Rous sarcoma virus; SDS, sodium dodecyl sulfate.

***Endocrinology* is published monthly by The Endocrine Society (http://www.endo-society.org), the foremost professional society serving the endocrine community.**

Materials and Methods

Materials

Secondary antibodies, as well as those against p-ERK, and ERK-1 were purchased from Santa Cruz Biotechnology Inc. (Santa Cruz, CA). The anti-LHβ antibody was purchased from National Institutes of Health (National Hormone Peptide Program, Torrance, CA; NIDDK-antirat-βLH-IC-2). Glass-bottom microwell dishes for confocal studies

were obtained from Mat-Tek (Ashland, MA). The adenovirus containing Rous sarcoma virus (RSV)-green fluorescent protein (GFP) was a generous gift from Dr. Wylie Vale (Salk Institute, La Jolla, CA). Jasplakinolide (Jas) and phorbol 12-myristate-13-acetate (PMA) were purchased from Calbiochem (La Jolla, CA). The low-melt agarose (type VII-A), GnRH, and antagonist (Antide) were obtained from Sigma (St. Louis, MO). Vitrogen was purchased from Cohesion Technologies (Palo Alto, CA). Transwells were purchased from Corning (Acton, MA). Alexa 594 or 488 conjugated phalloidin was purchased from Molecular Probes (Eugene, OR).

Animals

Mice were maintained on a 14-h light,10-h dark cycle with free access to rodent chow and water. For pituitary dissection, mice were anesthetized with ketamine (80 mg/kg) and xylazine (8 mg/kg) anesthesia. Ewes were maintained in pens with ambient lighting and free access to alfalfa and water. For pituitary dissection a follicular phase ewe was killed under pentobarbital anesthesia. All experiments were carried out in accordance with the National Institutes of Health Guide for the Care and Use of Laboratory Animals and the Colorado State University Animal Care and Use Committee.

Cell culture

αT3-1 cells were maintained in high-glucose (4.5 g/liter) DMEM containing 2 mM glutamine, 100 U/ml penicillin, 100 μg/ml streptomycin and 1× nonessential amino acids (Mediatech, Herndon, VA), with 5% fetal bovine serum and 5% horse serum (Gemini Bioproducts, Woodland, CA). αT3-1 cells were grown in 5% CO_2 in air at 37 C in a humidified environment.

Phalloidin staining

αT3-1 were grown in a 10-cm dish containing six glass coverslips coated with Matrigel (1:100; BD Biosciences, San Jose, CA). Before treatment with 100 nM GnRH and at various time points afterward, one coverslip was removed from the dish and immediately fixed by submersion in 4% paraformaldehyde in PBS for 20 min at room temperature. The coverslips were then rinsed twice with PBS and permeabilized for 10 min in 0.5% Triton X-100/PBS. After permeabilization, coverslips were rinsed twice with PBS and blocked in 1% BSA/PBS for 20 min at room temperature. Five microliters of Alexa-594 phalloidin were diluted in 200 μl 1% BSA/PBS and applied to the cells for 20 min at room temperature. Coverslips were then washed three times with PBS and mounted on slides using Poly-mount (Polysciences, Inc., Warrington, PA). Slides were imaged 48 h later using confocal laser-scanning microscopy (CLSM). The same procedure was followed for LβT2 imaging except that the cells were plated on Matrigel (1:100 dilution) coated glass-bottom microwell dishes and Alexa 488 phalloidin was used instead of Alexa 594 phalloidin.

Ovine pituitary dissociation

A follicular phase ewe was killed with an overdose of sodium pentobarbital, and the pituitary gland was removed aseptically. The pituitary was rinsed free of blood and cells dispersed enzymatically using collagenase, hyaluronidase, and deoxyribonuclease at 37 C for 90 min as previously described (18). Dissociated cells were then suspended in culture medium [DMEM supplemented with 10% horse serum (Gemini Bio-Products, Inc.), 2.5% fetal bovine serum, 1% nonessential amino acids, 100 IU/ml penicillin, and 100 μg/ml streptomycin]. Cells (1×10^6) in 2 ml media were plated in glass-bottom microwell dishes and cultured for 2 d at 37 C in a humidified atmosphere of 5% CO_2.

ERK activation assays

A monolayer of αT3-1 cells (2×10^5) in six-well tissue culture plates were washed twice with PBS and incubated in serum-free DMEM for 3 h. After serum starvation, cells were treated in the presence or absence of 1 μM Jas for 30 min. Either vehicle (0.1% dimethylsulfoxide), 100 nM GnRH, or 100 nM PMA was administered for 30 min. Cells were washed in ice-cold PBS and lysed in radioimmunoprecipitation assay buffer containing 20 mM Tris (pH 8.0), 137 mM NaCl, 10% glycerol, 1% Nonidet P-40, 0.1% sodium dodecyl sulfate (SDS), 0.5% deoxycholate, and 0.2 mM phenylmethylsulfonyl fluoride. Then 6 × sample buffer [300 mM Tris-HCl (pH 6.8), 60% glycerol, 30 mM DTT, 6% SDS] was added to yield a final concentration of 1×. Aliquots (15 μl) of each lysate were heated to 95 C for 5 min and subjected to SDS-PAGE and Western analysis. Nitrocellulose membranes were incubated for 2 h with a phospho-ERK antibody (1:1000 dilution) followed by a 2-h incubation with a 1:2000 dilution of horseradish peroxidase-conjugated secondary antibody. Phospho-ERK blots were then stripped at room temperature with 100 mM 2-mercaptoethanol, 2% SDS, and 62.5 mM Tris-HCl (pH 6.7) and heated to 50 C for 30 min. After stripping, membranes were washed twice for 15 min with Tris-buffered saline and blocked with 5% milk for 1 h and then reprobed with a 1:10,000 dilution of an anti-ERK-1 antibody that recognizes ERK-1 and ERK-2 independent of phosphorylation state. After washing in Tris-buffered saline, blots were incubated with a 1:2000 dilution of antirabbit horseradish peroxidase and immunoreactive bands were visualized by chemiluminescence.

Ex vivo slice preparation

Ex vivo slice preparation was similar to that previously reported (19). Murine pituitaries were dissected in cold Krebs' solution (NaCl 12.6 mM; KCl 0.25 mM; $CaCl_2$ 0.25 mM; $MgCl_2$ 0.12 mM; NaH_2PO_4 0.12 mM; glucose 11 mM; $NaHCO_3$ 25 mM) and embedded in 8% agarose (type VII-A; Sigma; maintained as liquid at 39 C) for sectioning at 200 μm in the horizontal plane. Slices intended for use in video microscopy were individually placed on glass-bottomed culture dishes (Mat Tek) that had been previously coated in poly-D-lysine and collagen (Vitrogen 100; Cohesion). Slices were infected with RSV-GFP using total viral titers of 4×10^9 (approximately 5 μl placed directly on top of the slice) and left for 1 h at 36 C at high humidity. Slices were then covered with more Vitrogen to prevent slice movements during video microscopy before the addition of the final media [glutamate supplemented phenol red-free Neurobasal + B27 supplement and penicillin (134 U/ml) and streptomycin (0.13 mg/ml)].

Video microscopy

For 1–3 d after infection, the slices were observed using time-lapse video microscopy. Images were acquired at 5-min intervals. Slices were maintained at 36–37 C for the duration of the video and supplied with continuous feed of 5% CO_2 in air. Images were captured on a TE-200 inverted microscope (Nikon, Tokyo, Japan) equipped with a 20 × Plan-Apo objective, Spot SE-6 interline transfer camera, and LUDL shutter system controlled by MetaMorph software (version 6.2; Universal Imaging Corp., Downingtown, PA). The system recorded three image planes spaced 5 μm apart, from which a maximal projection image was used to visualize fluorescing cells in a focal range covering 10 μm. To establish a baseline of motion, 1.5 h of time-lapse video was recorded for each slice before the addition of GnRH. PBS vehicle was also added at the beginning of each 30 min of baseline to control for effects of mechanical stimulation. After this period of baseline video, slices were treated with GnRH peptide every 30 min at a final concentration of 100 nM for up to 2 h. After viewing, each slice was fixed in 4% paraformaldehyde for at least 15 min at room temperature and stored in 0.1 M phosphate buffer until used for immunocytochemistry (ICC).

Video analysis

Images were analyzed for the presence of moving cells using the built-in z-projection and point tracking packages of MetaMorph (Universal Imaging). To track whole-cell motion, the center of each cell of interest was marked for each frame throughout the entire video sequence. Major characteristics of interest described in more detail previously (19) were the velocity, frequency of qualifying movement (velocity greater than 12 μm/h), and frequency of turning behavior. To quantify process extension, a line was drawn across the greatest distances between any two points on the border of the cell of interest for each frame. Frame-to-frame differences in line length reflect process extension or retraction. Characteristics of interest were speed of extension/retraction, total and maximum distance of extension, and probability of extension related to treatment.

Whole-mount ICC

The immunocytochemical procedures were as described previously (19). Briefly, slices were first pretreated to enhance permeability and decrease background. Slices were then exposed to an anti-LHβ antibody (1:1250) in 0.05M PBS containing 5% normal goat serum and 0.3% Triton X-100 for at least 6 d. For visualization, slices were incubated overnight with CY3-conjugated anti-guinea pig IgG secondary antibodies (1:500). After washing in PBS, slices were mounted on glass slides and coverslipped using VectaShield mounting media (Vector Laboratories, Burlingame, CA) for fluorescence viewing.

Modified Boyden chamber assay (transwells)

Dissociated ovine pituitary cells were incubated in serum-free medium for 2 h and harvested with 1 × trypsin. After centrifugation, the cell pellet was suspended in serum-free DMEM and 100,000 cells were seeded in the upper chamber of the transwell. For those wells that received GnRH treatment, 100 nM GnRH were added to cells in the upper chamber. Lower chambers were administered serum-free DMEM or serum-free DMEM containing 100 nM GnRH. Each treatment was done in duplicate for each of three replicates. Cells were then incubated overnight in 5% CO_2 at 37 C in a humidified environment. Analysis of cell migration was performed as previously described (20).

Statistical analysis

Data (see data in Fig. 7) and values reported for serum concentrations of LH were analyzed by paired *t* test (proc: *t* test) (SAS Institute, Cary, NC) with alpha = 0.05. Data (see data in Fig. 6) were analyzed by repeated-measures ANOVA for baseline *vs.* time periods after GnRH treatment (one time point for cell movements and three for processes). Because data were not collected for later time points for every cell when examining cell motion, a one-way ANOVA comparing across time points was also used.

Results

GnRH binding leads to rapid and transient morphological changes in αT3-1 cells

We (21) previously constructed an αT3-1 cell line that stably expresses an enhanced yellow florescent protein (CLONTECH, Palo Alto, CA) tagged GnRHR. In this analysis, cells were imaged by CLSM before GnRH treatment (Fig. 1A) and at 1-min intervals for 35 min after addition of GnRH (100 nM). Within 1 min of treatment, profound changes in membrane topography were evident as promi-

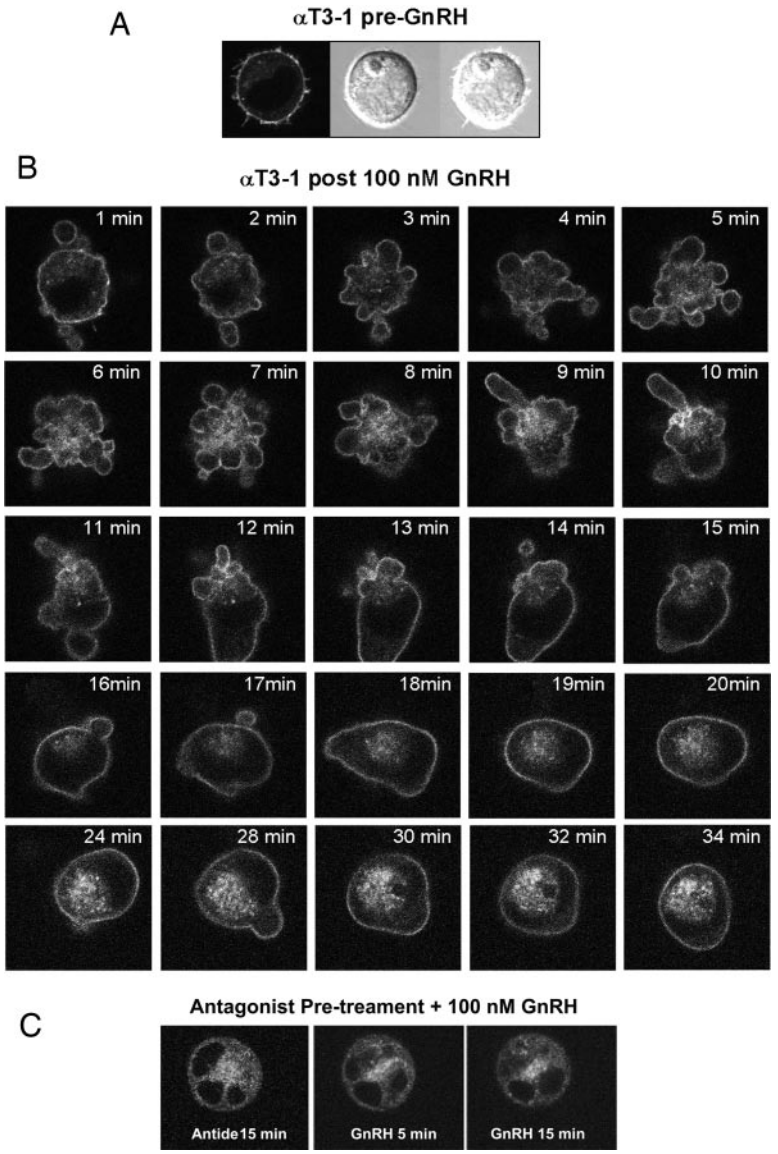

FIG. 1. GnRH leads to rapid and transient morphological changes in the αT3-1 gonadotrope-derived cell line. A, αT3-1 cells stably expressing an enhanced yellow fluorescent protein (eYFP) tagged GnRHR (GnRHR-YFP) were imaged by CLSM before GnRH treatment and at 60-sec intervals for 35 min after GnRH (100 nM) administration (B). C, αT3-1 cells stably expressing GnRHR-YFP were treated with 10 nM Antide and images were taken every 60 sec for 15 min using CLSM. After 15 min of Antide, a 100-nM GnRH challenge was administered. Again, images were taken every 60 sec for 15 min using CLSM.

nent blebs (Fig. 1B) reminiscent of nonapoptotic membrane blebbing in locomoting cells (22, 23). These changes were, however, transient and cells returned to pretreatment morphology within 15–30 min. This effect of GnRH was specific to the biologically active peptide because the GnRH antagonist Antide had no impact on membrane remodeling. Additionally, subsequent GnRH administration was unable to elicit any change in cellular architecture. Thus, these changes were specific to GnRH and the GnRH receptor (Fig. 1C).

GnRH-induced rearrangement is mediated by the actin cytoskeleton

Engagement of the actin cytoskeleton is a likely mechanism underlying the effects of GnRH on cell movements. To examine this, monolayers of αT3-1 cells were plated on glass coverslips, treated with either vehicle or 100 nM GnRH for 10 min fixed with 4% paraformaldehyde, and stained with Alexa 594-conjugated phalloidin. After GnRH treatment, rapid actin remodeling was evident as the formation of prominent stress fibers (Fig. 2A). Consistent with actin cytoskeletal mediated movement, pretreatment with a pharmacological disruptor of the actin cytoskeleton, jasplakinolide, blocked the GnRH-mediated morphological rearrangements (Fig. 2B). Thus, GnRH binding to the GnRHR activates signaling events that rapidly culminate in engagement of the actin cytoskeleton. Engagement of the actin cytoskeleton has been implicated as a requisite event in MAPK activation by multiple G protein-coupled receptors (17, 24). To test this in our system, αT3-1 cells were serum starved for 3 h and then treated in the presence or absence of 1 μM Jas for 30 min before GnRH (100 nM) or PMA (100 nM) treatment. Consistent with earlier studies (25–27), both GnRH and PMA induced ERK phosphorylation in control cells. In contrast, Jas pretreatment resulted in a loss of GnRH-induced ERK phosphorylation. Importantly, however, Jas pretreatment did not visibly compromise ERK activation in response to PMA. Thus, actin disruption with Jas interrupts GnRH but not PMA signaling to ERK (Fig. 2C). To ensure that GnRH mediated actin remodeling was not unique to the αT3-1 cell line, we repeated this analysis in LβT2 cells. This cell line is also

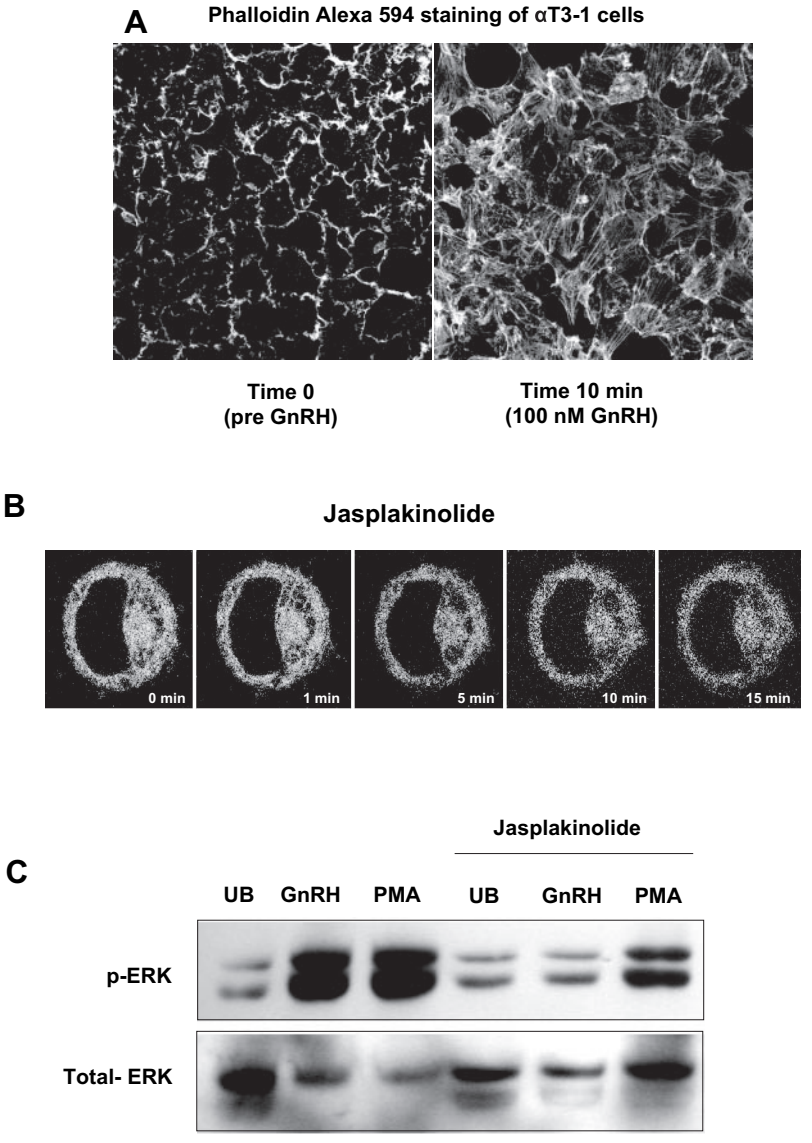

FIG. 2. GnRH-induced changes in cellular morphology are mediated by the actin cytoskeleton. A, αT3-1 cells were grown on glass coverslips, treated in the presence or absence of 100 nM GnRH for 10 min, and then fixed in 4% paraformaldehyde. Cells were then permeabilized and stained with Alexa 594-conjugated phalloidin, mounted on slides, and imaged using CLSM. B, αT3-1 cells stably expressing a GnRHR-YFP were pretreated for 30 min with 1 μM Jas. Cells were imaged by CLSM immediately before and after treatment with GnRH (100 nM). Images were taken every 60 sec after the administration of GnRH for up to 15 min. C, Serum-starved αT3-1 cells were treated for 30 min in the presence or absence of 1 μM Jas. Cells were then administered vehicle (0.1% dimethylsulfoxide), 100 nM GnRH, or 100 nM PMA for 30 min. Samples were then lysed in radioimmunoprecipitation assay buffer and lysates analyzed by Western blotting using antibodies specific for phosphorylated ERK. After probing with anti-phospho-ERK, blots were stripped and reprobed with an antibody that detects ERK-1 and -2 independent of phosphorylation. UB, Unbound.

of gonadotrope origin but, unlike αT3-1 cells, expresses the LHβ subunit gene (28). Consistent with the αT3-1 data, GnRH treatment of LβT2 cells led to actin remodeling; however, the formation of lamellipodia and cellular extensions was more evident in these cells (Fig. 3)

Cell processes form after GnRH treatment of pituitary cell primary cultures

The data above demonstrate that GnRH engagement of the actin cytoskeleton leads to transient morphological changes of transformed αT3-1 and LβT2 cells (Figs. 1 and 3). To assess the effects of GnRH on *bona fide* pituitary cells, primary cultures of ovine pituitary cells were established as previously described (18). A large field of dissociated pituitary cells was imaged using the differential interference contrast (DIC) channel of an LSM 510 confocal microscope (Zeiss, New York), and GnRH (100 nM) was then added. For cells that responded with morphological changes, images were collected every 60 sec for 30 min. GnRH treatment led to formation of cell processes (marked by *arrows*) that extended as much as 1 cell diameter (Fig. 4). A video sequence of this cell behavior is available online as supplemental material (published as supplemental data on The Endocrine Society's Journals Online Web site at http://endo.endojournals.org; see accompanying movie file).

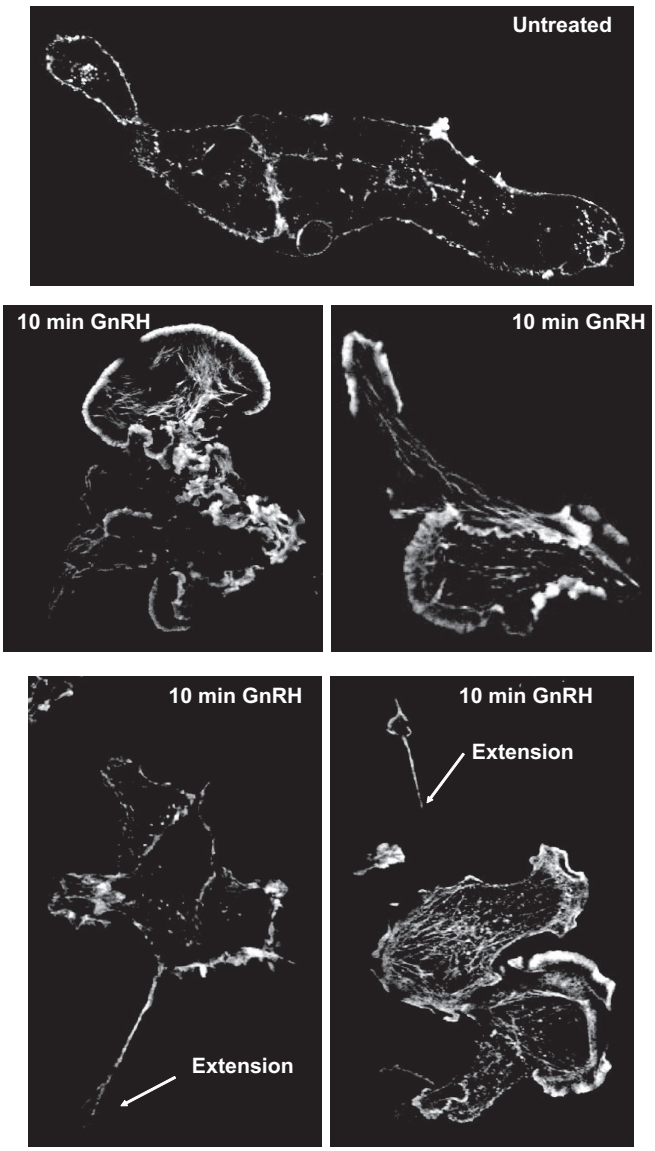

FIG. 3. GnRH leads to actin remodeling in the gonadotrope derived LβT2 cell line. LβT2 cells were grown on coated glass-bottom microwell dishes, incubated in the presence or absence of 100 nM GnRH for 10 min, and then fixed in 4% paraformaldehyde. Cells were then permeabilized, stained with Alexa 488-conjugated phalloidin, and imaged by CLSM.

GnRH stimulates the formation of cell processes and spatial repositioning in ex vivo pituitary slices

The *in vitro* data (Fig. 4) confirm the ability of GnRH to stimulate the formation of processes in dissociated pituitary cells. To determine whether this type of movement is also evident in intact murine pituitaries, we used an *ex vivo* paradigm with live pituitary slices. We adapted a developmental brain slice approach (19) to the pituitary, preparing 200-μm-thick sections adhered to coverslip surfaces and viewed using inverted epifluorescence optics. In Fig. 5A, a phase image demonstrates the morphological integrity of the 200-μm-thick pituitary slice from an adult mouse. To directly visualize cells within the murine pituitary, we used an adenoviral construct in which enhanced GFP (eGFP; CLONTECH) expression was placed under transcriptional control of the constitutive RSV promoter (RSV-GFP). As an initial test of the utility of adenovirus in the pituitary slice paradigm, purified, high-titer viral stocks were prepared and then slices were infected with total viral titers of 4×10^9 PFU. After infection, slices were viewed at 24 and 48 h after infection to assess eGFP expression levels (Fig. 5B). To assess whether this approach resulted in infection of gonadotropes, slices were fixed and processed for immunoreactive LHβ using a Cy-3-labeled secondary antibody (Fig. 5C). Images were obtained with a Zeiss LSM 510 confocal microscope using the ×40 objective and the 488 and 543 laser lines. Based on colocalization (overlay of *red* and *green* signals is presented as *yellow*) of eGFP and immunoreactive LHβ (Cy-3 *red* signal), gonadotropes were susceptible to infection and support expression of eGFP (Fig. 5D).

To assess the functional viability of the pituitary slices, a RIA was used to investigate the production of LH in response to GnRH treatment. After 1 h of baseline imaging (no GnRH), incubation medium was harvested and replaced with fresh culture medium. GnRH (100 nM) was then administered for 1 h, and again medium was collected and replaced. Medium samples were then analyzed for the concentration of LH using RIA as previously described (29). LH concentrations were approximately 3-fold higher in media obtained from pituitary slices after 1 h of GnRH treatment (25 ± 1.41 ng/ml), compared with baseline (7.5 ± 1.95 ng/ml) ($P < 0.05$). Thus, the functional integrity of GnRH-induced gonadotropin secretion was retained in pituitary slices.

To directly observe the dynamics of GnRH stimulated cell motion in living pituitary slices, images of RSV-GFP infected murine pituitaries were collected every 5 min during a baseline period (no GnRH treatment) and after 90 min of GnRH

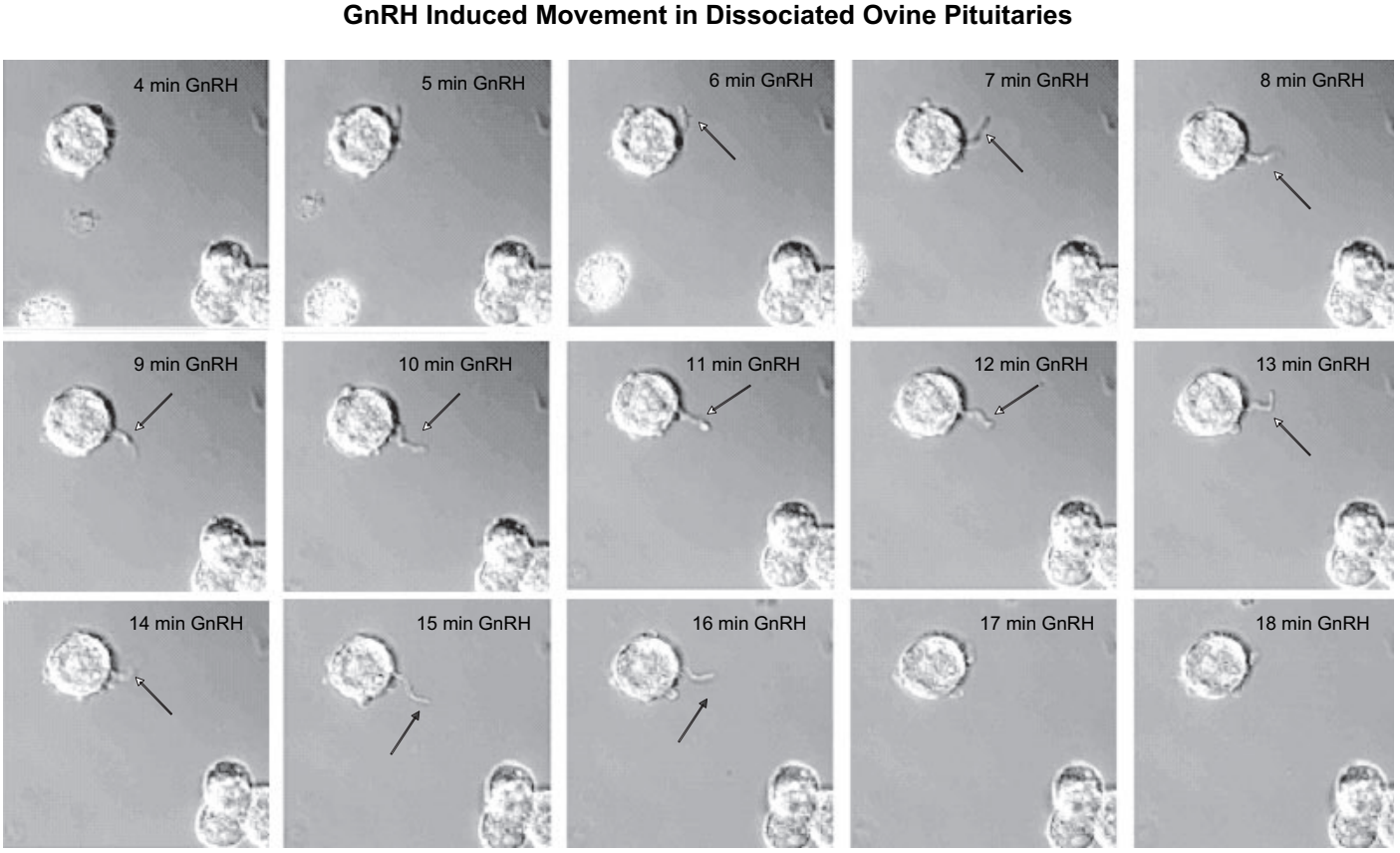

FIG. 4. GnRH treatment of pituitary cells in primary culture stimulates the formation of cellular processes. Primary cultures of dissociated ovine pituitary cells were incubated for 24 h and then treated with 100 nM GnRH for the indicated times. Images were acquired using CLSM in DIC mode. *Arrows* indicate the formation of a cellular process in a responding cell.

(100 nM) treatment. Remarkably we found that GnRH treatment led to not only cell process formation but also spatial repositioning of cells. *Solid arrows* mark two eGFP-labeled cells of interest in baseline video (Fig. 6A). *Dashed arrows* mark the location and process formation of the same eGFP-labeled cells after the administration of 100 nM GnRH for 60 min (Fig. 6B). GnRH treatment led to a pronounced increase in both the rate of movement and net distance moved of a small subset of eGFP cells in the analyzed field. GnRH treatment also led to a dramatic increase in process formation in a different subset of eGFP-labeled cells (Fig. 6C). The effects of GnRH were reversed with treatment with the GnRH antagonist Antide (10 nM) (data not shown). A video sequence showing this cell behavior in slices is available on line as supplemental material (see accompanying movie file).

The process formation in the *ex vivo* pituitary slice is consistent with the cellular motion evident in the LβT2 cell line and the dissociated pituitary cells (Figs. 3 and 4); however, the whole cell movement leading to spatial repositioning in the pituitary was entirely unexpected and suggests that GnRH-responsive cells possess an intrinsic capacity to migrate. To test GnRH influences on pituitary cell migration in a different setting, we used modified Boyden chambers (transwells) with dissociated ovine pituitary cells in the presence or absence of GnRH (100 nM) in serum-free DMEM. Consistent with the *ex vivo* data, when cells were incubated in the presence of GnRH, there was an 8-fold increase ($P <$ 0.01) in the number of cells that crossed the transwell membrane (Fig. 7). These results indicate that pituitary cells can respond to GnRH by at least two types of distinct cellular motion including process formation and cell movement.

Discussion

Given the central role of GnRH in reproduction, much effort has been devoted toward understanding the physiological consequences of regulating GnRH secretion from the brain and its receptor in the pituitary. Toward this end, we found that GnRH binding leads to rapid and transient morphological changes in the gonadotrope-derived αT3-1 cell line. Importantly, when antagonist treatment was followed with GnRH (100 nM), movement was abrogated. These findings demonstrate that the actions of GnRH were mediated through GnRHR signaling.

Our data suggest that GnRH-induced cell movements are mediated by the actin cytoskeleton, a result consistent with the ability of GnRH to lead to actin reorganization in HEK293 cells (17) and prostate cancer cell lines (30). It is interesting that in both HEK293 cells and the pituitary-derived αT3-1 cell line, GnRH-induced actin assembly not only mediates cell movements but also appears to be fundamental to GnRH signaling to the level of MAPK activation. Thus, gonadotrope movement and intracellular signaling are linked to GnRH engagement of the actin cytoskeleton. At present it is not

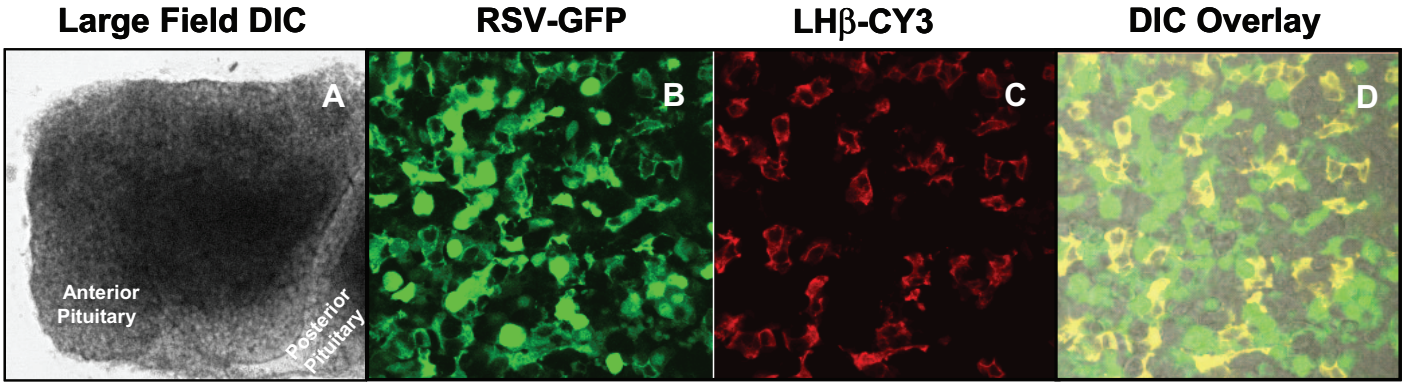

FIG. 5. GFP expression is detectable in gonadotropes using adenoviral-mediated gene transfer. A, A large field DIC image was taken of the murine pituitary slice before imaging. B, Murine pituitary slices were prepared and infected with adenovirus containing RSV-GFP as described in *Materials and Methods*. C, After live slice imaging, pituitary slices were fixed in 4% paraformaldehyde and subjected to ICC for the β-subunit of LH (LHβ) using a CY-3 conjugated secondary antibody. D, Colocalization of the *green* (GFP) and *red* (LH staining) signals is evident as *yellow* in the overlay of the DIC images.

entirely clear at what level these cellular events are linked; however, several points can be made. First, it is clear that ERK activation itself is not required for GnRH engagement of the actin cytoskeleton and that pharmacological bypass of the GnRHR using phorbol ester leads to ERK activation in an actin-independent fashion (data not shown). Thus, ERK activation is functionally downstream of GnRH-mediated actin reorganization. Second, we established that the GnRHR is localized to low-density microdomains termed lipid rafts, and raft localization of the GnRHR is essential for signaling to ERK (16). Third, Davidson *et al.* (17) suggested that GnRH signaling to the actin cytoskeleton and ERK is via integrin-mediated activation of focal adhesion kinase in membrane focal adhesion complexes. Importantly, integrins and focal adhesions have been implicated in recruitment of Rho family members to membrane lipid rafts, an event that appears to underlie not only cytoskeletal engagement and migration but also polarity and cell movement along a chemotactic gradient

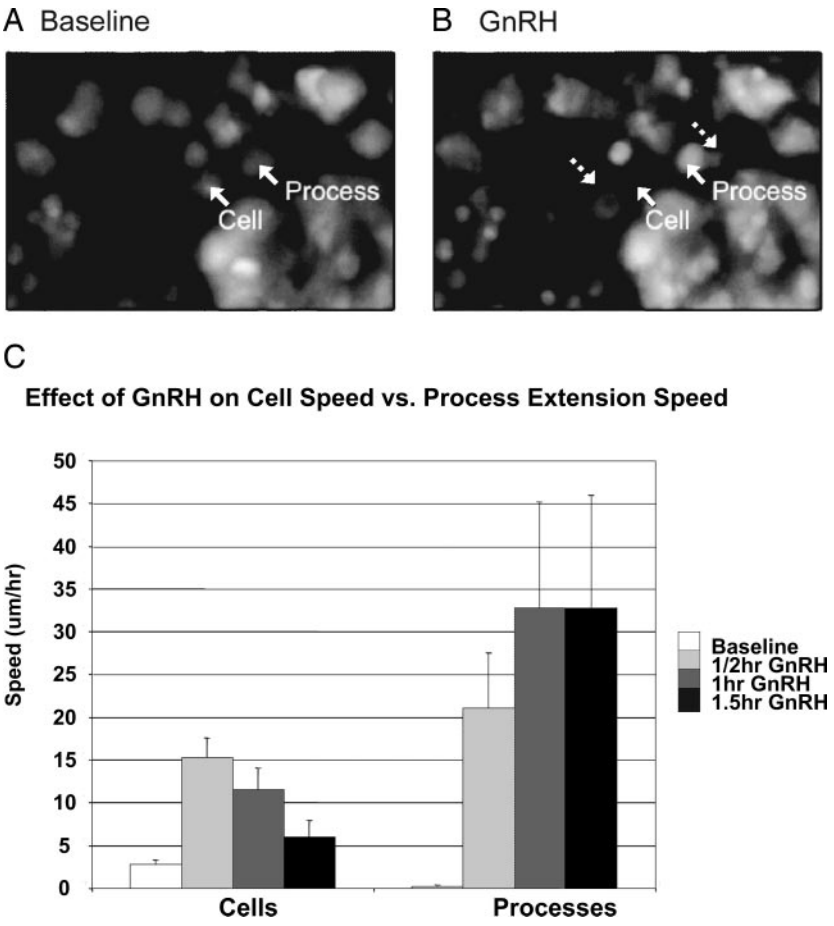

FIG. 6. GnRH treatment increased the rate of movement and net distance moved of adenoviral infected RSV-GFP cells in live pituitary slices. A, Murine pituitary slices were prepared and infected with an adenovirus containing RSV-GFP as in Fig. 5. Movement of GFP-labeled cells was observed directly using time-lapse video microscopy and movements were analyzed using MetaMorph image analysis software. *Solid arrows* mark GFP-labeled cells in the absence of GnRH. *Dashed arrows* mark the final location and process formation of the same GFP-labeled cells 60 min after 100 nM GnRH treatment (B). The video sequence is available as supplemental material. The graph (C) shows that movements of cell bodies increased significantly after GnRH exposure (repeated measures ANOVA comparing baseline with 30 min exposure: $F(1, 21) = 28.5, P < 0.001$) and then desensitized after 60 min. The movement of processes, however, continued over the full 90-min observation period (repeated measures ANOVA comparing baseline and three time periods of exposure: $F(3, 18) = 4.3, P < 0.02$). Data depicted are means ± SEM.

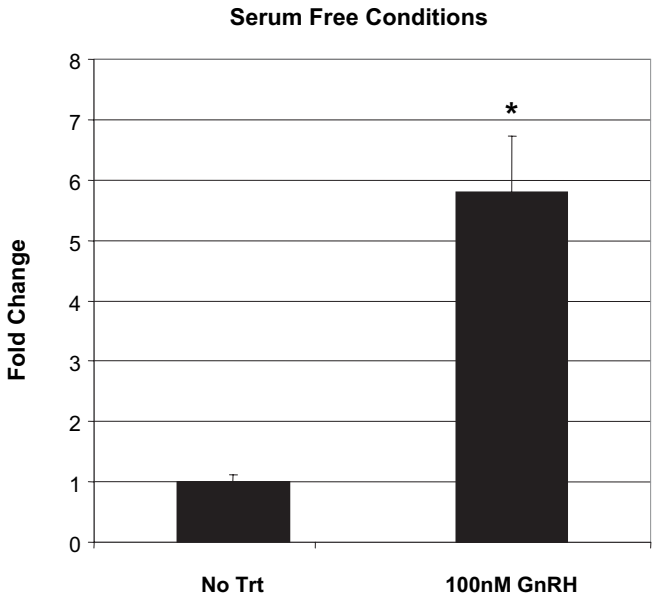

FIG. 7. GnRH treatment increased the number of dissociated ovine pituitary cells migrating in transwell chambers. Dissociated ovine pituitary cells were serum starved for 2 h and placed in the upper chamber of the transwell at a concentration of 100,000 cells per 0.1 ml in serum-free medium. Serum-free medium or serum-free medium containing 100 nM GnRH was placed in the lower chamber of the transwells. Cells in the upper chamber of the transwells were incubated in the presence or absence of GnRH (100 nM) overnight. Each treatment was performed in duplicate. After overnight incubation, cells were washed and stained with crystal violet for 30 min. Cells remaining in the upper chamber were removed with a cotton swab and the filters were removed. Cells that migrated to the bottom of the filter were mounted with coverslips and counted using a hemocytometer. *Error bars* represent SEM with three replicates. *, $P < 0.01$. Trt, Treatment.

(31–34). Thus, lipid rafts may serve as the most proximate platform for organizing GnRHR signaling to actin and ERK. Consistent with this notion, depletion of cellular cholesterol sufficient to lead to raft disruption resulted in the loss of GnRH signaling to ERK (16) and dissociated cell movements (data not shown). Finally, in terms of cell locomotion, it is interesting to note that the membrane blebbing induced by GnRH treatment of the gonadotrope-derived αT3-1 cell line is similar to membrane behaviors associated with apoptosis; however, nonapoptotic membrane blebbing has been implicated as a mode of cell locomotion in both transformed and nontransformed cells (22, 23).

In the current study, GnRH-mediated changes in cellular architecture were recapitulated in *bona fide* pituitary cells. We found that dissociated ovine pituitary cells can respond to GnRH with process formation. Our current results, however, further suggest that pituitary cells are capable of whole cell movements in response to GnRH. In other systems, studies have shown actin-dependent migration of human prostate cancer cell lines in response to GnRH (30). Our results with video microscopy, cell lines, transwell chambers, and dissociated cells show that GnRH is capable of inducing process formation and cell migration in anterior pituitary cells.

To better understand pituitary cell movements in the context of an intact gland, we adopted an *ex vivo* pituitary slice paradigm that allowed us to directly visualize pituitary plasticity *in situ*. An important finding of this study is that GnRH treatment of living pituitary slices led to a pronounced increase in both the rate of movement and net distance moved of eGFP-labeled cells. Thus, these data demonstrate two distinct hormone-induced changes in movement of endocrine cells in the anterior pituitary gland. It is not likely that these cell movements are a futile or random expenditure of energy. We propose that these GnRH-responsive cells are moving to appose themselves to vascular endothelium, thus gaining more immediate access to the bloodstream for hormone release from the basolateral membrane. This hypothesis is not without precedent. Childs (7) noted that GnRH-stimulated gonadotropes developed processes and, later, that these processes extended to blood vessels during peak LH secretory episodes (8). A similar suggestion lies in a striking series of static three-dimensional reconstructions of pituitary vasculature and corticotrophs (35, 36). The current live imaging data in cells and slices place an exclamation mark on the potential for a greater extent of plasticity with particular vascular targets. We recognize that the ability of cells to move through extracellular matrices often requires matrix remodeling via the activity of members of the matrix metalloproteinase (MMP) family. Importantly, GnRH treatment of the gonadotrope-derived αT3-1 cell line leads to release of active MMP2 and MMP9 and enhances the gelatinolytic activity of these enzymes within 5 min of treatment (37). Thus, gonadotropes appear to possess an intrinsic capacity for matrix remodeling that is responsive to GnRH input.

In summary, we have used video microscopy in three different paradigms, immortalized pituitary cells, primary dissociated pituitary cells, and live pituitary slices to demonstrate GnRH-induced cell movement evident as both cellular repositioning and extension of cellular processes. Contrary to current dogma, our data suggest that the adult pituitary displays significant plasticity that is evident as not only cellular process formation but also whole cell movements.

Acknowledgments

The authors thank Drs. Margaret E. Wierman and Sheila Neilsen-Preiss for their help in establishing the cell migration assay in Transwell chambers.

Received August 21, 2006. Accepted December 29, 2006.

Address all correspondence and requests for reprints to: Colin M. Clay, Colorado State University, Department of Biomedical Sciences, 1683 Campus Delivery, Fort Collins, Colorado 80523. E-mail: colin.clay@colostate.edu.

This work was supported by National Science Foundation Grant NSF0534608.

Author Disclosure Summary: A.M.N., J.G.K., J.D.W., S.A.T., and C.M.C. have nothing to declare.

References

1. **Keogh EJ, Meakin JL, Banovic S, Curnow DH, Giles PH, Clarke IJ, Wilson JD** 1983 Ovulation induction with pulsatile gonadotrophin releasing hormone (GnRH). Clin Reprod Fertil 2:175–189
2. **Brinkley HJ** 1981 Endocrine signalling and female reproduction. Biol Reprod 24:22–43
3. **Clayton RN, Catt KJ** 1981 Gonadotropin-releasing hormone receptors: characterization, physiological regulation and relationship to reproductive function. Endocr Rev 2:186–209
4. **Gharib SD, Wierman ME, Shupnik MA, Chin WW** 1990 Molecular biology of the pituitary gonadotropins. Endocr Rev 11:177–190

5. **Counis R, Laverriere JN, Garrel G, Bleux C, Cohen-Tannoudji J, Lerrant Y, Kottler ML, Magre S** 2005 Gonadotropin-releasing hormone and the control of gonadotrope function. Reprod Nutr Dev 45:243–254
6. **Childs GV, Unabia G, Lloyd J** 1992 Recruitment and maturation of small subsets of luteinizing hormone gonadotropes during the estrous cycle. Endocrinology 130:335–344
7. **Childs GV** 1998 Gonadotropes. In: Knobil E, Neill JD, eds. Encyclopedia of reproduction. San Diego: Academic Press; 498–506
8. **Childs GV** 1985 Shifts in gonadotropin storage in cultured gonadotropes following GnRH stimulation, *in vitro*. Peptides 6:103–107
9. **Childs GV, Unabia G, Lee BL, Rougeau D** 1992 Heightened secretion by small and medium-sized luteinizing hormone (LH) gonadotropes late in the cycle suggests contributions to the LH surge or possible paracrine interactions. Endocrinology 130:345–352
10. **Lloyd JM, Childs GV** 1988 Differential storage and release of luteinizing hormone and follicle-releasing hormone from individual gonadotropes separated by centrifugal elutriation. Endocrinology 122:1282–1290
11. **Kaiser UB, Conn PM, Chin WW** 1997 Studies of gonadotropin-releasing hormone (GnRH) action using GnRH receptor-expressing pituitary cell lines. Endocr Rev 18:46–70
12. **Stanislaus D, Janovick JA, Brothers S, Conn PM** 1997 Regulation of G(q/11)α by the gonadotropin-releasing hormone receptor. Mol Endocrinol 11:738–746
13. **Roberson MS, Misra-Press A, Laurance ME, Stork PJS, Maurer RA** 1995 A role for mitogen-activated protein kinase in mediating activation of the glycoprotein hormone α-subunit promoter by gonadotropin-releasing hormone. Mol Cell Biol 15:3531–3539
14. **Weck J, Fallest PC, Pitt LK, Shupnik MA** 1998 Differential gonadotropin-releasing hormone stimulation of rat luteinizing hormone subunit gene transcription by calcium influx and mitogen-activated protein kinase-signaling pathways. Mol Endocrinol 12:451–457
15. **White BR, Duval DL, Mulvaney JM, Roberson MS, Clay CM** 1999 Homologous regulation of the gonadotropin-releasing hormone receptor gene is partially mediated by protein kinase C activation of an activator protein-1 element. Mol Endocrinol 13:566–577
16. **Navratil AM, Bliss SP, Berghorn KA, Haughian JM, Farmerie TA, Graham JK, Clay CM, Roberson MS** 2003 Constitutive localization of the gonadotropin-releasing hormone (GnRH) receptor to low-density membrane microdomains is necessary for GnRH signaling to ERK. J Biol Chem 278:31593–31602
17. **Davidson L, Pawson AJ, Millar RP, Maudsley S** 2004 Cytoskeletal reorganization dependence of signaling by the gonadotropin-releasing hormone receptor. J Biol Chem 279:1980–1993
18. **Gregg DW, Allen MC, Nett TM** 1990 Estradiol-induced increase in number of gonadotropin-releasing hormone receptors in cultured ovine pituitary cells. Biol Reprod 43:1032–1036
19. **Tobet SA, Walker HJ, Seney ML, Yu KW** 2003 Viewing cell movements in the developing neuroendocrine brain. Integr Comp Biol 43:794–801
20. **Allen MP, Linseman DA, Udo H, Xu M, Schaack JB, Varnum B, Kandel ER, Heidenreich KA, Wierman ME** 2002 Novel mechanism for gonadotropin-releasing hormone neuronal migration involving Gas6/Ark signaling to p38 mitogen-activated protein kinase. Mol Cell Biol 22:599–613
21. **Nelson S, Horvat RD, Malvey J, Roess DA, Barisas BG, Clay CM** 1999 Characterization of an intrinsically fluorescent gonadotropin-releasing hormone receptor and effects of ligand binding on receptor lateral diffusion. Endocrinology 140:950–957
22. **Cunningham CC** 1995 Actin polymerization and intracellular solvent flow in cell surface blebbing. J Cell Biol 129:1589–1599
23. **Pirone DM, Fukuhara S, Gutkind JS, Burbelo PD** 2000 SPECs, small binding proteins for Cdc42. J Biol Chem 275:22650–22656
24. **Dutt P, Kjoller L, Giel M, Hall A, Toksoz D** 2002 Activated Galphaq family members induce Rho GTPase activation and Rho-dependent actin filament assembly. FEBS Lett 531:565–569
25. **Reiss N, Llevi LN, Shacham S, Harris D, Seger R, Naor Z** 1997 Mechanism of mitogen-activated protein kinase activation by gonadotropin-releasing hormone in the pituitary of αT3-1 cell line: differential roles of calcium and protein kinase C. Endocrinology 138:1673–1682
26. **Mulvaney JM, Zhang T, Fewtrell C, Roberson MS** 1999 Calcium influx through L-type channels is required for selective activation of extracellular signal-regulated kinase by gonadotropin-releasing hormone. J Biol Chem 274:29796–29804
27. **Liu F, Austin DA, Mellon PL, Olefsky JM, Webster NJG** 2002 GnRH activates ERK1/2 leading to the induction of *c-fos* and LHβ protein expression in LβT2 cells. Mol Endocrinol 16:419–434
28. **Thomas P, Mellon PL, Turgeon J, Waring DW** 1996 The LβT2 clonal gonadotrope: a model for single cell studies of endocrine cell secretion. Endocrinology 137:2979–2989
29. **Niswender GD, Midgley ARJ, Monroe SE, Reichert LEJ** 1968 Radioimmunoassay for rat luteinizing hormone with antiovine LH serum and ovine LH-131-I. Proc Soc Exp Biol Med 128:807–811
30. **Enomoto M, Utsumi M, Park MK** 2006 Gonadotropin-releasing hormone induces actin cytoskeleton remodeling and affects cell migration in a cell-type-specific manner in TSU-Pr1 and DU145 cells. Endocrinology 147:530–542
31. **Wang HR, Zhang Y, Ozdamar B, Ogunjimi AA, Alexandrova E, Thomsen GH, Wrana JL** 2003 Regulation of cell polarity and protrusion formation by targeting RhoA for degradation. Science 302:1775–1779
32. **Dustin ML** 2002 Shmoos, rafts, and uropods—the many facets of cell polarity. Cell 110:13–18
33. **Palazzo AF, Eng CH, Schlaepfer DD, Marcantonio EE, Gundersen GG** 2004 Localized stabilization of microtubules by integrin- and FAK-facilitated Rho signaling. Science 303:836–839
34. **Hoekstra D, Maier O, van der Wouden JM, Slimane TA, van Ijzendoorn SC** 2003 Membrane dynamics and cell polarity: the role of sphingolipids. J Lipid Res 44:869–877
35. **Itoh J, Kawai K, Serizawa A, Yasumura K, Ogawa K, Osamura RY** 2000 A new approach to three-dimensional reconstructed imaging of hormone-secreting cells and their microvessel environments in rat pituitary glands by confocal laser scanning microscopy. J Histochem Cytochem 48:569–578
36. **Itoh J, Serizawa A, Kawai K, Ishii Y, Teramoto A, Osamura RY** 2003 Vascular networks and endothelial cells in the rat experimental pituitary glands and in the human pituitary adenomas. Microsc Res Tech 60:231–235
37. **Roelle S, Grosse R, Aigner A, Krell HW, Czubayko F, Gudermann T** 2003 Matrix metalloproteinases 2 and 9 mediate epidermal growth factor receptor transactivation by gonadotropin-releasing hormone. J Biol Chem 278:47307–47318

***Endocrinology* is published monthly by The Endocrine Society (http://www.endo-society.org), the foremost professional society serving the endocrine community.**